Research on the jet characteristics of the deflector–jet mechanism of the servo valve*

Hao Yan(延皓)†, Feng-Ju Wang(王凤聚), Chang-Chun Li(李长春), and Jing Huang(黄静)

School of Mechanical, Electronic and Control Engineering, Beijing Jiaotong University, Beijing 100044, *China*

(Received 9 October 2016; revised manuscript received 13 November 2016; published online 20 February 2017)

In view of the complicated structure of the deflector–jet mechanism, a mathematical model based on the turbulent jet flow theory in the deflector–jet amplifier is proposed. Considering the energy transformation and momentum variation, an equation of the flow velocity distribution at the key fluid region is established to describe the morphological changes of the fluid when it passes through the deflector and jets into the receiver. Moreover, the process is segmented into four stages. According to the research results, the oil enters the deflector and impinges with the side wall. Then one part of the oil's flow velocity decreases and a high pressure zone is formed by the oil accumulation, the other part of the oil reverses out of the deflector along the side wall. Prior to entering the receiver, the flow is a kind of plane impinging jet. Virtually, the working pressure of the receiver is generated by the impact force, while the high speed fluid flows out of the receiver and forms a violent vortex, which generates negative pressure and causes the oil to be gasified. Compared with the numerical simulation results, the turbulent jet model that can effectively describe the characteristics of the deflector–jet mechanism is accurate. In addition, the calculation results of the prestage pressure characteristic have been verified by experiments.

Keywords: servo valve, prestage, turbulent jet, deflector jet

PACS: 47.60.Kz, 47.85.Dh, 47.27.wg **DOI:** 10.1088/1674-1056/26/4/044701

1. Introduction

Deflector jet servo valves[1] have the characteristics of a strong antipollution ability and wide utilization in various types of actuator and control systems in the fields of aerospace, national defense, and civil aircraft. The deflector jet amplifier (Fig. 1) is a precise and complex component, which can change the jet status of the fluid by a tiny creeping of the deflector and affect the pressure of the two receivers.[2]

Because of the similarity, the research method of the flow field of the deflector jet valve is always rooted in the jet pipe valve. Somashekhar[3] established an accurate jet pipe valve model which was based on the throttling theory and the fluid-structure interaction model of the jet pipe valve was built by the finite element method to simulate the complete working process of the jet pipe valve. In the study of Pham,[4,5] a mathematical model of the prestage of the jet pipe valve was established, which was applied to obtain the characteristics of the prestage. Li[6] and Shang[7] studied the recovery pressure and flow velocity in the receiving port based on the characteristics analysis of the flow field, then the optimal structure parameters are obtained. According to the computational fluid dynamics (CFD) and the erosion theory, the influence of the different structures on the erosion are studied by Yin.[8] Chu[9] studied the erosion wear rate in the receiver of jet pipe servo valves by building a two-phase flow numerical model, then a calculation method for the life span of jet pipe serve valves was proposed.

On the basis of jet pipe valve research, exploiting the throttle principle in the circular jet exit and considering the throttle area's change, Wang[10] proposed a linearized flow equation. Yin[11,12] summarized the effect of receivers' dimension, oil pressure and other parameters on the pressure characteristic and flow field of the prestage. By means of simulation and experiment, the influence of the geometry of the receiver on the flow distribution was analyzed by Yang.[13] Ma[14] gained the conclusion that greater pressure can be obtained by using the wedge structure, which was consistent with Yang's results. The key parameters of the torque motor and spool valve were designed by Jiang,[15] who presented an innovative analysis of the internal flow field of the pilot valve by the turbulent jet theory and impinging jet theory. The new type of deflector jet servo valve was announced in the United States Patent US2006216167,[16] which enhanced the performance of the servo valve by innovating the structure of the feedback rod in the prestage. Furthermore, Dhinesh[17] designed a new type of servo valve based on double piezoelectric crystal, which had a significant improvement in the performance of the valve. With the application of giant magnetostrictive material (GMM) to drive the deflector, another type of servo valve was developed by Li,[18] which had the characteristics of fast response and high pressure gain. As stated previously, the current research on the deflector jet servo valve mainly focuses on the analysis of the whole dynamic characteristics and the flow field description. Most of the theoretical models are based on the circular jet exit and receivers, only considering the flow field between the jet disk and the receiv-

*Project supported by the International Science and Technology Cooperation Program of China (Grant No. 2012DFG71490).

†Corresponding author. E-mail: bjtujd@163.com

© 2017 Chinese Physical Society and IOP Publishing Ltd

ing port, what are developed from throttle theory. Although it simplifies the analysis process, it is not consistent with the actual situation obviously. There is no complete theoretical model to describe the key flow field which has not been analyzed and calculated accurately. In addition, some scholars studied the flow in similar conditions.[19–22]

According to the complex structure of the deflector jet mechanism, this paper presents a complete mathematical model which is based on the turbulent jet theory. Finally, numerical simulations of the flow field and the pressure characteristic experiment of the prestage are utilized to verify the validity of the model.

2. Description of the whole flow process

Based on the complex structure of the pilot valve, a model is built to describe the turbulent flow reasonably, where the working process is divided into four stages: initial jet, deflector pressure recovery, deflector jet, and receiver pressure recovery. The process can be described as Fig. 1.

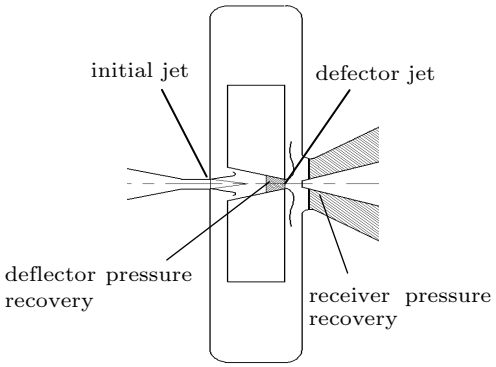


Fig. 1. Structure of plane turbulent jet.

The oil flowing from the nozzle is called the initial jet before contacting with the deflector. Then the velocity of the fluid decreases and a high pressure zone forms as a result of the contact between oil and deflector, which is known as deflector pressure recovery. A deflector jet represents that the oil jets again from the deflector. The last one is described as a process of receiver pressure recovery, in which another high pressure zone is formed at the two receivers.

3. Model of deflector jet amplifier

3.1. Velocity distribution of the initial jet

In the steady-state flow, the fluid pressure can be completely converted into kinetic energy. The ideal Bernoulli equation for fluid flow along the streamline can be expressed as

$$p_0 = \frac{1}{2}\rho {u_0}^2, \tag{1}$$

where p_0 is the system initial pressure, ρ is the hydraulic oil density, and u_0 is the velocity of the oil at the nozzle. $u_0 = 219.72$ m/s can be obtained from Eq. (1). Thus the initial jet is a free turbulent jet in the deflector jet amplifier.

The structure of the free turbulent jet[23] is shown in Fig. 2. The fluid velocity in the core zone is not affected by the stationary fluid around and keeps the original velocity.

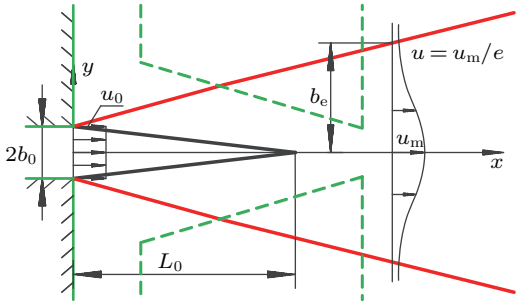


Fig. 2. (color online) Structure of plane turbulent jet.

The coordinate system is established and the dotted line is the contour of the deflector, as is shown in Fig. 2. Momentum flux remains constant in the planar turbulent jet, thus

$$M = \int_{-\infty}^{\infty} \rho u^2 \,\mathrm{d}y, \tag{2}$$

in which u is the velocity of the oil at any section. The initial momentum in the jet exit is

$$M_0 = 2\rho u_0^2 b_0, \tag{3}$$

where b_0 is the width of the initial jet exit. Then equation (4) can be obtained by the conservation of momentum

$$\int_{-\infty}^{\infty} \rho u^2 \,\mathrm{d}y = 2\rho u_0^2 b_0. \tag{4}$$

Forthmann's experimental data[24] show that there is velocity similarity in the main section of the turbulent jet. The boundary of the jet flow is defined where the oil velocity is equal to u_m/e, and the half thickness is b_e. At this time, the mean velocity distribution in the main section of planar turbulent jet accords with the following Gaussian distribution,

$$\frac{u}{u_m} = \exp\left(-\frac{y^2}{{b_e}^2}\right). \tag{5}$$

Substituting the velocity distribution Eq. (5) into Eq. (2), we can obtain

$$\int_{-\infty}^{\infty} \rho u^2 \,\mathrm{d}y = \rho\sqrt{\frac{\pi}{2}} u_m^2 b_e \tag{6}$$

and

$$\rho\sqrt{\frac{\pi}{2}} u_m^2 b_e = 2\rho u_0^2 b_0. \tag{7}$$

According to the linear expansion of the jet thickness, $b_e = \varepsilon x$ can be assumed, which can be put into Eq. (7) and the decay of velocity along the centerline can be expressed as

$$\frac{u_m}{u_0} = \left(\sqrt{\frac{2}{\pi}}\frac{1}{\varepsilon}\right)^{1/2}\left(\frac{2b_0}{x}\right)^{1/2}, \tag{8}$$

where x is the coordinate along the center line. Combined with Alberson's experiment result that $\varepsilon = 0.154$, the velocity distribution can be obtained

$$u_{\mathrm{m}} = 2.28\sqrt{\frac{2b_0}{x}}u_0. \tag{9}$$

Obviously, the velocity along the center line is inversely proportional to the square root of the distance to the jet source. According to Eq. (5), the velocity of the jet of any cross section can be calculated by

$$u = 2.28\sqrt{\frac{2b_0}{x}}u_0 \exp\left[-\left(\frac{y}{b_{\mathrm{e}}}\right)^2\right]. \tag{10}$$

Moreover, the length of the core area $L_0 = b_0/\tan\theta = 10.4b_0$, where θ is the external expansion angle of the initial jet.

The results of the calculation show that the core area has stretched into the V-shaped slot of the deflector, so the collision between the jet and the deflector is still in the initial section of the jet. Actually, the potential core is terminated in advance due to the effect of the side walls of the deflector, which means the jet flow has gone into the main section.

3.2. Back flow and deflector pressure recovery

The pressure recovery of the deflector is shown in Fig. 3. In any cross section of the initial jet before the contact between the jet and the deflector, the total mean kinetic energy is

$$\begin{aligned} E &= 2\int_0^{\infty}\frac{u^2}{2}\rho u\,\mathrm{d}y \\ &= \int_0^{\infty}\rho\left(2.28\sqrt{\frac{2b_0}{x}}u_0\right)^3\exp\left[-3\left(\frac{y}{b_{\mathrm{e}}}\right)^2\right]\mathrm{d}y. \end{aligned} \tag{11}$$

The coordinate of the contact point is represented by x_c, which can be calculated by the structure of the deflector jet amplifier and the external expansion angle $\theta = 10^\circ$. Then $x_c = 0.47$ mm can be obtained.

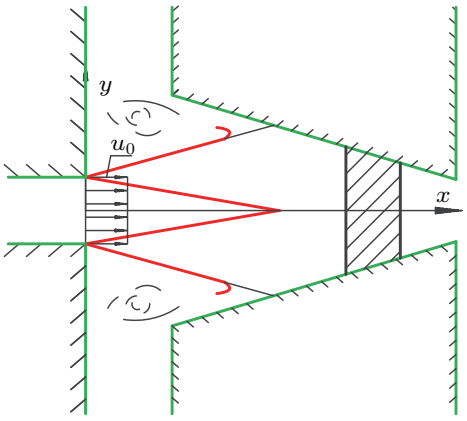


Fig. 3. (color online) Deflector pressure recovery.

With the interaction of the fluid and the deflector, there will be part of the oil flowing back, which means that some fluid will carry kinetic energy out of the deflector.

As shown in the following Fig. 4, there will be a wall attachment effect on the fluid in the triangular area, causing the oil to flow back.

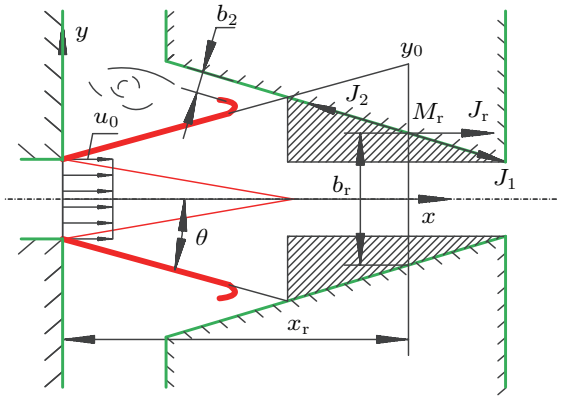


Fig. 4. (color online) The collision of the jet and the deflector.

According to Bourque and Newman's wall attachment jet model[25] and the conservation law of momentum,

$$J_0\cos(\theta) = J_1 - J_2 \tag{12}$$

and

$$J_0 = J_1 + J_2, \tag{13}$$

where J_1 is the momentum of the fluid flowing into the high-pressure zone along the deflector side wall, J_2 is the momentum of the fluid flowing back from the deflector and J_0 is the initial momentum of the jet. According to their definition, we can learn that

$$J_1 = \int_0^{y_{\mathrm{r}}}\rho u^2\,\mathrm{d}y,\ J_2 = \int_{y_{\mathrm{r}}}^{y_0}\rho u^2\,\mathrm{d}y,\ J_0 = \rho u_0^2 b_0.$$

y_{r} are the vertical coordinates of the point M_{r}.

From Eqs. (12) and (13), the distance from the Point M_{r} on the side wall to the jet exit is obtained, that is, $x_{\mathrm{r}} = 0.527$ mm. Then $b_{\mathrm{r}} = 0.323$ mm, which is the width of Point M_{r}'s section and can be calculated by the geometric parameters of the deflector.

Supposing that the flow energy is constant and the momentum is conserved, the velocity u_2 and the thickness b_2 of the backflow can be obtained by Eqs. (12), (13), and (14), which are respectively computed with the results that $u_2 = 84.59$ m/s and $b_2 = 0.031$ mm.

$$\rho b_2 u_2^2 = \int_{y_{\mathrm{r}}}^{y_0}\rho u^2\,\mathrm{d}y. \tag{14}$$

The kinetic energy of the fluid flowing into the high pressure zone will be converted to pressure energy because of the extrusion from the side wall, forming a high pressure area. The pressure can be calculated by the energy conservation law. The high pressure zone is shown in Fig. 5.

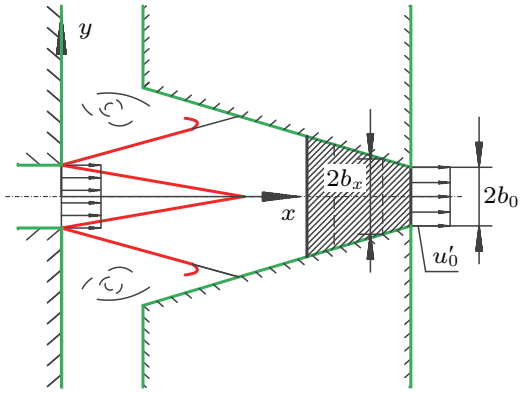


Fig. 5. (color online) The high pressure zone of the deflector.

The flow of the deflector exit is also simplified to a free turbulent jet with a uniform velocity u'_0. The velocity can be calculated by

$$\rho b'_0 u'^2_0 = \int_0^{y_r} \rho u^2 \mathrm{d}y. \tag{15}$$

Then, $u'_0 = 173.07$ m/s. Assuming that the flow velocity in any section is approximately uniform, the continuity equation can be constructed, i.e.,

$$2b_x u_x = 2b'_0 u'_0, \tag{16}$$

where b_x is the width of the section and u_x is the flow velocity in the section. The velocity of the fluid of the point M_r's section are calculated, i.e., $u_r = 75.06$ m/s.

Meanwhile, the pressure on any section can be calculated by Bernoulli equation

$$\frac{1}{2}\rho u'^2_0 = p_x + \frac{1}{2}\rho {u_x}^2. \tag{17}$$

The pressure p_r at point M_r is highest in the pressure recovery zone, i.e.,

$$p_r = \frac{1}{2}\rho u'^2_0 - \frac{1}{2}\rho {u_r}^2 = 10.58 \text{ MPa}. \tag{18}$$

Obviously, with the fluid approaching the deflector jet exit, the flow velocity increases and the pressure drops.

3.3. Deflector jet and receiver pressure recovery

Considering the law of conservation of energy and ignoring the energy loss of the flow, the kinetic energy of the fluid passing through the deflector can be expressed as

$$E'_0 = \rho b_0 u'^3_0. \tag{19}$$

Assuming that the fluid is incompressible, since the oil flowing into the two receivers is unable to flow out, the deflector jet acts directly on the oil surface and the shunt structure in the receiver, similar to an impinging jet, as is shown in Fig. 6.

Actually, the fluid in the receiver is subjected to the shearing action of the impinging fluid, which generates a turbulent mixing, causing part of the fluid to be swirled and flow into the receiver. Compared with the jet fluid flowing out of the receiver, this part of the flow is little and can be ignored.

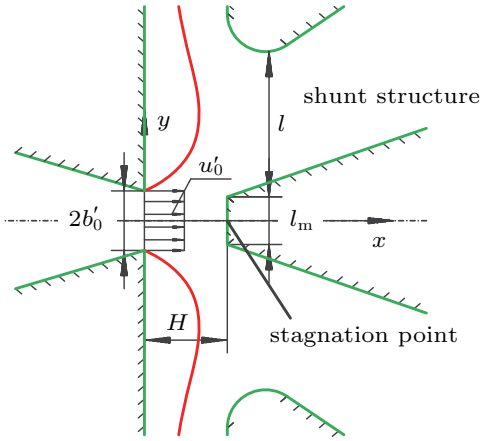


Fig. 6. (color online) Deflector jet.

According to the pressure distribution of the impinging jet and the momentum theorem in the jet's direction, the jet's impingement force on the wall can be obtained by

$$2\rho b'_0 u'^2_0 - 2\int_0^{l_m/2} p\mathrm{d}y = (p_1 + p_2)l, \tag{20}$$

where p_1, p_2 are the pressures of two receiving ports, l is the width of each receiving port and l_m is the length of the shunt structure. The maximum pressure on the shunt structure is p_s, which is known as the stagnation point pressure and can be described by

$$\frac{p_s}{\rho(u'^2_0/2)} \cdot \frac{H}{2b'_0} = \text{const.}, \tag{21}$$

where H is the distance between the deflector jet exit and the receiving port. The const is obtained by simulation, as shown in Table 1.

Table 1. The constant of impinging jet.

Jet distance/mm	Maximum pressure/MPa	Const.
0.05	19.3	0.5421
0.10	17.0	0.9550
0.15	16.7	1.4072
0.195	16.3	1.7745
0.25	15.8	2.2189
0.30	15.4	2.5954

The actual jet distance H is 0.195 mm, so the maximum pressure and the const can be obtained, that is, $p_s = 16.3$ MPa and const. ≈ 1.77. The coordinate system is established in Fig. 6. Consider a cross section of the jet, the pressure on the axis is p_m and the pressure at the other position is p, then we can obtain

$$\frac{p_m}{p_s} = 3.2\frac{x}{H} - 2.2, \tag{22}$$

$$\frac{p}{p_{\mathrm{m}}} = \exp\left[-\left(\lambda\frac{y}{b_{\mathrm{p}}}\right)^2\right], \tag{23}$$

where b_{p} is the jet width when $p = \frac{1}{2}p_{\mathrm{m}}$. From the experimental data,[26] we can obtain that $b_{\mathrm{p}} = 0.134H$ and $\lambda = 0.835$. From Eqs. (20), (22), and (23), the pressure of the receiver is 3.8 MPa when the deflector is in the center. The relative displacement between the deflector and the receiving port is represented by x_{f}. Then the pressure of the two receiving ports can be expressed as

$$p_1 = \frac{1}{l}\rho b_0' u_0'^2 - \frac{p_{\mathrm{s}}}{l}\int_0^{l_{\mathrm{m}}/2-x_{\mathrm{f}}} \exp\left[-\left(\lambda\frac{y}{b_{\mathrm{p}}}\right)^2\right]\mathrm{d}y, \tag{24}$$

$$p_2 = \frac{1}{l}\rho b_0' u_0'^2 - \frac{p_{\mathrm{s}}}{l}\int_0^{l_{\mathrm{m}}/2+x_{\mathrm{f}}} \exp\left[-\left(\lambda\frac{y}{b_{\mathrm{p}}}\right)^2\right]\mathrm{d}y. \tag{25}$$

Finally, the pressure gain can be determined by

$$K_{\mathrm{p}} = \frac{p_1 - p_2}{x_{\mathrm{f}}} = \frac{p_{\mathrm{s}}\int_{l_{\mathrm{m}}/2-x_{\mathrm{f}}}^{l_{\mathrm{m}}/2+x_{\mathrm{f}}} \exp\left[-\left(\lambda\frac{y}{b_{\mathrm{p}}}\right)^2\right]\mathrm{d}y}{lx_{\mathrm{f}}}. \tag{26}$$

4. Computation and analysis of the model

4.1. The kinetic energy and flow rate of the initial jet

The deflector jet mechanism's geometrical parameters are substituted into Eqs. (27) and (28), which express the relative kinetic energy E_{j} and relative flow rate Q_{j} of any section in the initial jet, as shown in Fig. 7.

$$E_{\mathrm{j}} = \frac{E}{E_0} = \int_0^{\infty} u^3\,\mathrm{d}y/b_0u_0^3, \tag{27}$$

$$Q_{\mathrm{j}} = \frac{Q}{Q_0} = \int_0^{\infty} u\,\mathrm{d}y/u_0b_0, \tag{28}$$

where E is the jet kinetic energy of any section, E_0 is the jet kinetic energy of the jet exit, Q is the flow rate of a section in the jet direction and Q_0 is the flow rate at the jet exit.

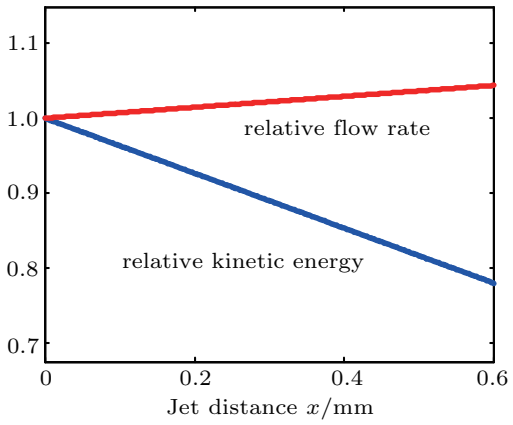


Fig. 7. (color online) Relative kinetic energy and flow rate of the initial jet.

The initial jet in the prestage is a free turbulent jet, so the flow rate increases linearly along the jet distance. In fact, the entrainment rate v_{e} and the entrainment coefficient α_{e} of the jet are both constant, which can be calculated by[27]

$$v_{\mathrm{e}} = \frac{1}{2}\frac{\mathrm{d}Q}{\mathrm{d}x}, \tag{29}$$

$$\alpha_{\mathrm{e}} = \frac{v_{\mathrm{e}}}{u_0} = \frac{1}{2u_0}\frac{\mathrm{d}Q}{\mathrm{d}x}. \tag{30}$$

Then, $v_{\mathrm{e}} = 2.3957$ m/s and $\alpha_{\mathrm{e}} = 1.12\%$.

The kinetic energy of the free turbulent jet decreases linearly with the raise of the jet distance. The loss rate of kinetic energy is 17.25% when the jet impacts the deflector, which can be obtained by Eq. (27).

$$K_{\mathrm{j}} = 1 - \frac{E}{E_0} = 1 - E_{\mathrm{j}}. \tag{31}$$

4.2. Pressure recovery in the deflector

In the process of the collision between the jet fluid and the deflector, the energy and the momentum conservation are considered in the small field.

After the collision, the pressure of the high pressure area can be calculated by the energy conservation principle. Figures 8 and 9 show the pressure and kinetic energy in the pressure recovery area.

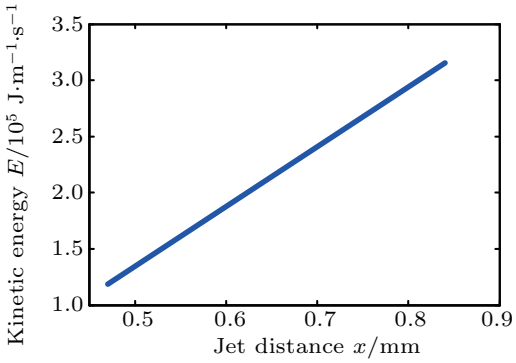


Fig. 8. (color online) The kinetic energy after the pressure recovery.

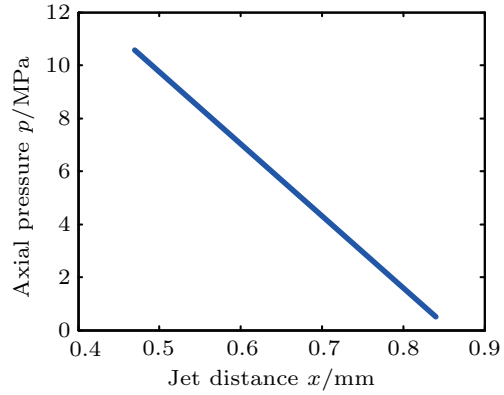


Fig. 9. (color online) The axial pressure after the pressure recovery.

The simulation results show that a high pressure will be generated after the collision between the jet and the deflector and the stagnation point pressure is 10.58 MPa. At this point, the kinetic energy reaches the minimum. Then the pressure

energy will be converted into kinetic energy, so the average kinetic energy increases and the pressure is reduced. Finally the fluid velocity becomes the initial velocity of the deflector jet and $u_0' = 173.07$ m/s. From Eq. (19), the kinetic energy of the deflector jet is 3.155×10^5 J/(m·s). And the original energy can be calculated, that is, $\rho b_0 u_0^3 = 6.170 \times 10^5$ J/(m·s). Then the energy loss ratio of the initial jet is 51.13%.

Obviously, the shape of the deflector determines the backflow pattern, so a U-shaped deflector can be designed to replace the current V-shaped structure. It can be expected that the return flow and the energy loss will decrease.

4.3. Pressure distribution in the deflector jet

From Eq. (23), the pressure distribution on the shunt surface (Fig. 7) is shown in Fig. 10. The pressure of the stagnation point is 15.7 MPa.

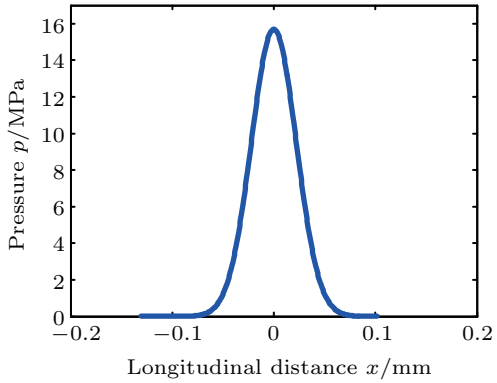


Fig. 10. (color online) The pressure distribution on the shunt surface.

5. Numerical simulation of deflector jet amplifier

The parameters of the simulation are shown in Table 2.

Table 2. Simulation parameters.

Parameter	Simulation value
Oil density/(kg/m^3)	849
Viscosity/kg/(m·s)	0.01305
Inlet pressure/MPa	21
Outlet pressure/MPa	0.5

5.1. Initial jet

Compared with the free turbulent jet, the core area of the initial jet is evidently affected by the deflector. The length of the core area is greatly shortened (as shown in Fig. 11). In fact, because of the influence of the deflector, the external expansion angle θ of the jet changes.

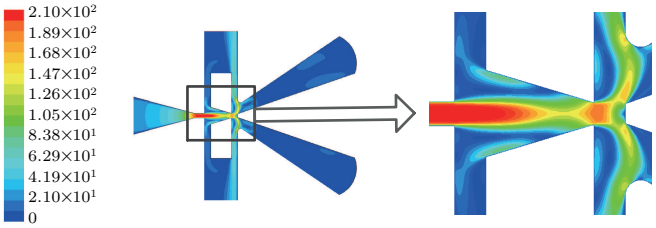


Fig. 11. (color online) Flow velocity distribution in the deflector.

5.2. Pressure distribution in deflector

The pressure distribution in the deflector is shown in Fig. 12. Obviously, the high pressure region appears in the deflector and the pressure gradually decreased with the approach to the deflector exit. Meanwhile, reflux part flows out of the deflector along the side wall and a finite space jet forms in the gap between the deflector and the initial jet exit, thereby producing vortexes and low pressure areas.

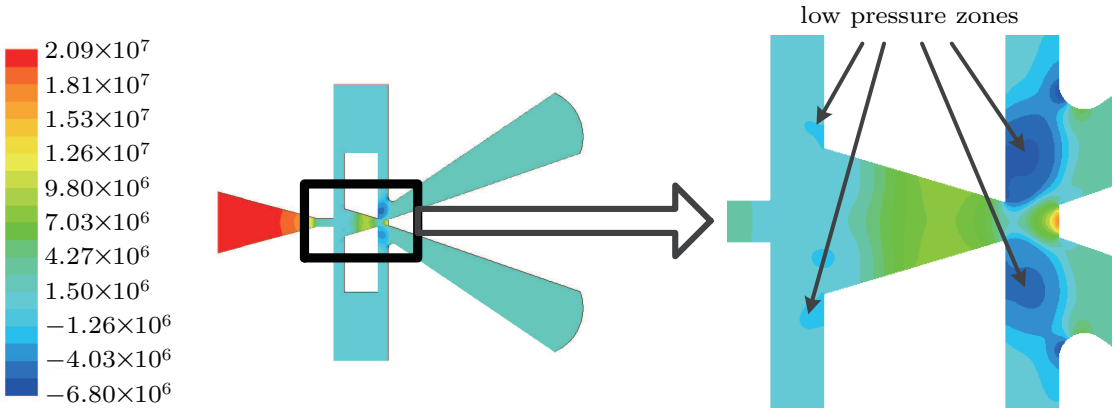


Fig. 12. (color online) Pressure distribution in deflector.

5.3. Deflector jet

The oil boundary in the receiving port is not a solid one, so the deflector jet will be poured into the receiving port before flowing out from both sides, which is different with the theoretical analysis, but the pressure distribution of the deflector jet is the same as the plane impinging jet. As shown in Fig. 13, the fluid flows out of the receiving port and generates more intense vortexes. Then negative pressure zones appear and the oil will be gasified.

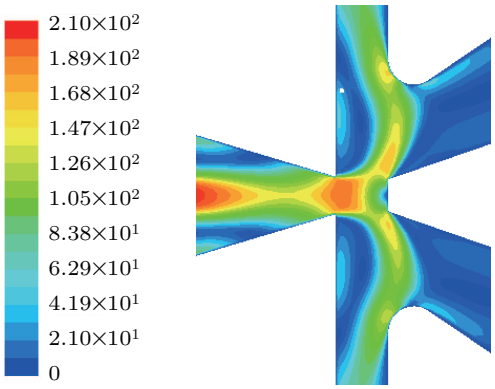


Fig. 13. (color online) Flow velocity distribution of the deflector jet.

5.4. Numerical simulation of deflector jet

The pressure distribution on the receiving port's shunt surface is shown in Fig. 14 when the displacement is 0, 0.01, 0.02, 0.03, 0.04, 0.05, 0.06, 0.07 mm.

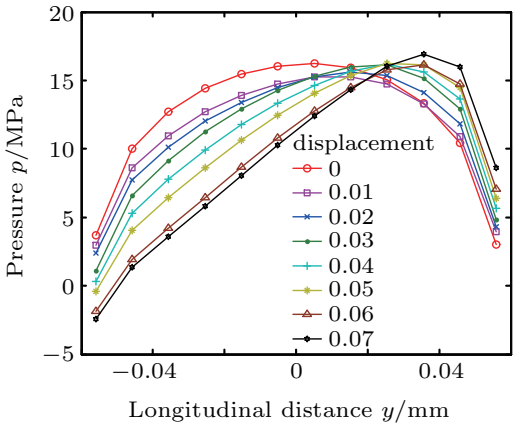


Fig. 14. (color online) The pressure distribution on the shunt surface.

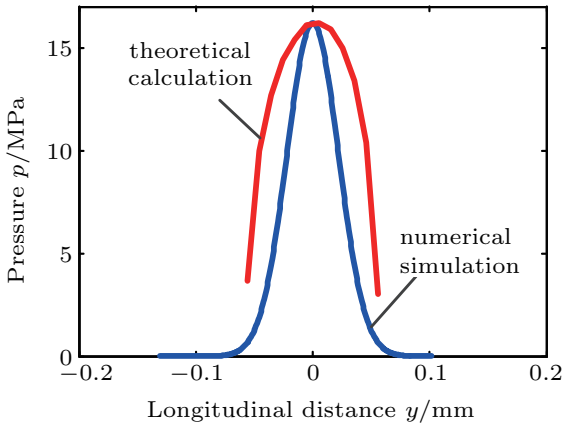


Fig. 15. (color online) Pressure distribution before the parameter modification.

The simulation indicates that the maximum pressure point of the platform moves to the right with the deflection plate's moving, but the maximum pressure value does not change significantly. The pressure distribution is similar to the Gauss distribution. Moreover, the deflector jet becomes an impinging jet after the contact with the shunt surface, which is consistent with the theoretical analysis. The pressure curves of the theoretical calculation and the numerical simulation are shown in Fig. 15 when the deflector is at the central position.

The results show that the theoretical distribution curve is more narrow than the simulated one, which illustrates the variable's coefficient λ in Eq. (23) is too large. As the available experimental data are derived from low-viscosity gas, λ needs to be amended. So we can suppose that $\lambda = 0.3$ and the curves are shown in Fig. 16.

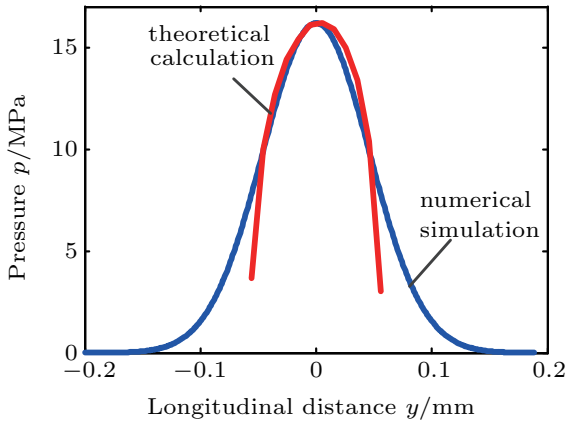


Fig. 16. (color online) Pressure distribution after the parameter modification.

According to Eqs. (24) and (25), the load pressure of the pilot valve is shown in Fig. 17. From Eq. (26), $K_p = 0.106$ MPa/μm.

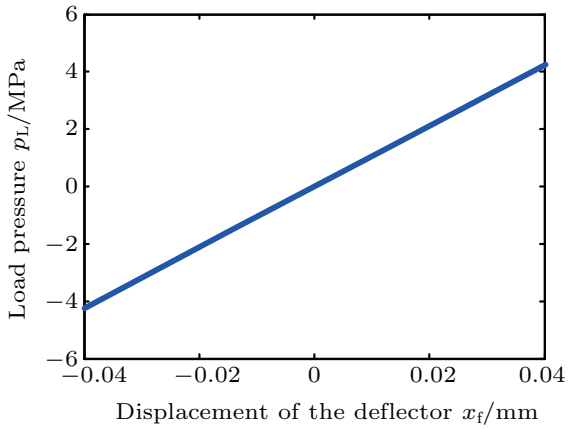


Fig. 17. (color online) Pressure distribution after the parameter modification.

6. Experiments

The theoretical calculation shows that the model is able to analytically describe the jet flow mechanism and quantitatively give theoretical mean value of key parameters; the numerical simulation essentially coincides with the computational result. Finally, the external characteristic experiments are carried out to verify the theoretical model with the experimental equipment in Fig. 18.

The upward extension of the torque motor is driven by the electric actuator, and the micro displacement is measured

by a laser sensor. According to the structure parameters of the jet mechanism, the displacement of the deflector can be calculated. Meanwhile, the pressure of the two receiving ports is measured. The experimental curve and the theoretical curve are shown in Fig. 19.

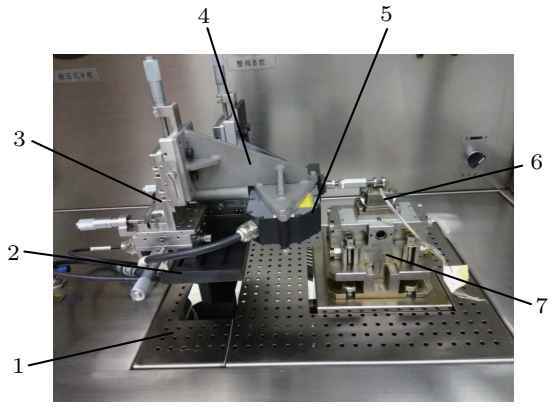


Fig. 18. (color online) External characteristics experiment of prestage. 1: Platform; 2: Adapter block; 3: Three-dimensional micro displacement worktable; 4: Laser sensor mounting bracket; 5: Laser sensor; 6: Servo valve; 7: Adapter block for servo valve.

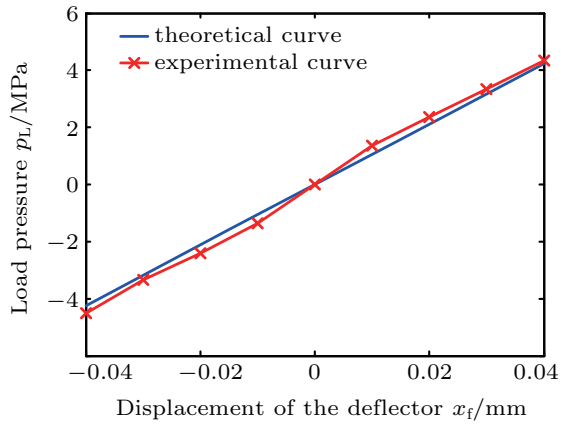


Fig. 19. (color online) Pressure distribution after the parameter modification.

The experimental results show that the pressure gain of the deflector jet mechanism is 0.118 MPa/μm and the deviation of the theoretical model is 0.012 MPa/μm. So the calculation results of the theoretical model are in agreement with the experimental results.

7. Conclusions

To sum up, we draw the following conclusions.

(i) The flow process in the deflector jet mechanism is a complex finite space jet. Consequently, a new mathematical model based on the jet theory is put forward. The flow process is divided into four stages and can be clearly described.

(ii) Theoretical analysis and numerical simulation show that after the collision between the initial jet and the deflector, a high pressure zone is formed and a considerable part of the fluid flows back from the deflector. Because of the backflow, the energy loss ratio of the initial jet is 51.13%, which means that the energy loss caused by the initial jet exceeds half of the total energy. On the other hand, the deflector jet can be approximately regarded as an impinging jet. The working pressure in the receiving port is provided by the jet impact force at the liquid surface.

(iii) Part of the fluid reflects from the deflector and becomes a limited space jet in the narrow gap between the deflector and the jet disk, resulting in vortexes and low pressure zones. Similarly, the deflector jet at the receiving port is also a kind of limited space jet, which brings more intense vortexes and negative pressure zones. Actually the oil will be drastically gasified.

(iv) Pressure distribution on the shunt surface is obtained by theoretical and numerical analysis. As the available experimental data are derived from low-viscosity gas, the parameter λ needs to be revised from 0.835 to 0.3 in order to apply the impinging jet law to the deflector jet. The modified theoretical results of the pressure characteristics of the deflector–jet mechanism are in agreement with the experimental results.

(v) Since the energy loss in the deflector jet mechanism is mainly caused by the backflow in the initial jet, a U-shaped deflector can be designed to replace the current V-shaped structure so that the return flow and the energy loss will be reduced.

References

[1] Mcfadden E F and Williams L J (U.S. Patent) 3 542 051 [1970-11-24]
[2] Wang C X 2011 *Hydraulic control systems* (Beijing: China Machine Press) pp. 103–104 (in Chinese)
[3] Somashekhar S H, Singaperumal M and Kumar R K 2006 *Proceedings of the Institution of Mechanical Engineers Part I: Journal of Systems & Control Engineering* **220** 109
[4] Pham X H S and Yin Y B 2012 *The 4th International Conference on Intelligent Human-Machine Systems and Cybernetics*, August 26–27, 2012, Nanchang, China, p. 310
[5] Pham X H S and Tran T P 2013 *Journal of Donghua University (Eng. Edn.)* **30** 269 (in Chinese)
[6] Li R P, Nie S L, Yi M L and Ruan J 2011 *Journal of Shanghai University* **15** 201
[7] Shang Y X, Zhang X S, Hu C W and Wu S 2015 *Machine Tool & Hydraulics* **43** 11
[8] Yin Y B, Fu J H and Jin Y L 2015 *Journal of Zhejiang University (Engineering Science)* **49** 2252
[9] Chu Y B, Yuan Z H and Zhang Y 2015 *Hangkong Xuebao Acta Aeronautica Et Astronautica Sinica* **36** 1548 (in Chinese)
[10] Wang C L, Ding F, Li Q P and Xu X L 2003 *Journal of Chongqing University* **26** 11 (in Chinese)
[11] Yin Y B, Zhang P and Cen B 2015 *Chinese Journal of Construction Machinery* **13** 1 (in Chinese)
[12] Yin Y B, Zhang P and Zhang Y 2014 *Fluid Power Transmission and Control* **4** 10 (in Chinese)
[13] Yang Y H 2006 "Analysis and Experimental Research of Prestage Jet Flow Field in Hydraulic Servo Valve", Master's Thesis (Harbin: Harbin Institute of Technology) (in Chinese)
[14] Ma Y F 2007 "Numerical simulation research of internal flow field of deflector jet hydraulic amplifier", Master's Thesis (Beijing: Minzu University of China) (in Chinese)
[15] Jiang L Q 2013 "Design and Research on a New Type of Deflection Plate Jet Servo Valve", Master's Thesis (Nanjing: Southeast University) (in Chinese)
[16] Muchlis Achmad (U.S. Patent) 7 290 565 [2007-06-11]

[17] Dhinesh K. Sangiah, Andrew R. Plummer, Christopher R. Bowen and Paul Guerrier 2011 *Dynamic Systems and Control Conference and Bath/ASME Symposium on Fluid Power and Motion Control*, October 31–November 2, 2011, Arlington, Virginia, USA, pp. 343–350
[18] Li Y S 2016 *Sensors & Actuators A: Physical* **245** 50
[19] Chen Z, Wu J H, Chen X, Lei H and Hou J J 2015 *Acta Phys. Sin.* **64** 054703 (in Chinese)
[20] Chen Y X, Chen K, You Y X and Hu T Q 2013 *Acta Phys. Sin.* **62** 114701 (in Chinese)
[21] Tu G Y, Li W F, Huang G F and Wang F C 2013 *Acta Phys. Sin.* **62** 084704 (in Chinese)
[22] Zhang Q, Chen X, He L M and Rong K 2013 *Acta Phys. Sin.* **62** 084706 (in Chinese)
[23] Stephen B Pope 2000 *Turbulent Flows* (New York: Cambridge University Press)
[24] Forthmann E 1936 *Technical Report Archive and Image Library*
[25] Bourque C and Newman B G 1960 *Aeronautical Quarterly* **11** 201
[26] Beltaos B and Rajaratnam N 1973 *Journal of Hydraulic Research* **11** 29
[27] Liu P Q 2008 *Free turbulent jet* (Beijing: Beijing University of Aeronautics and Astronautics Press) (in Chinese)